PRAMANA — journal of physics

© Indian Academy of Sciences

Vol. 82, No. 4
April 2014
pp. 757–767

Deformed shell model studies of spectroscopic properties of ^{64}Zn and ^{64}Ni and the positron double beta decay of ^{64}Zn

R SAHU[1,*] and V K B KOTA[2,3]

[1]Physics Department, Berhampur University, Berhampur 760 007, India
[2]Physical Research Laboratory, Ahmedabad 380 009, India
[3]Department of Physics, Laurentian University, Sudbury, ON P3E 2C6, Canada
*Corresponding author. E-mail: rankasahu@rediffmail.com

DOI: 10.1007/s12043-014-0726-5; ***e*Publication:** 5 April 2014

Abstract. The spectroscopic properties of ^{64}Zn and ^{64}Ni are calculated within the framework of the deformed shell model (DSM) based on Hartree–Fock states. GXPF1A interaction in $1f_{7/2}$, $2p_{3/2}$, $1f_{5/2}$ and $2p_{1/2}$ space with ^{40}Ca as the core is employed. After ensuring that DSM gives good description of the spectroscopic properties of low-lying levels in these two nuclei considered, nuclear transition matrix elements (NTME) for the neutrinoless positron double beta decay ($0\nu\beta^+\beta^+$ and $0\nu\beta^+$EC) of ^{64}Zn are calculated. The two-neutrino positron double beta decay half-life is also calculated for this nucleus.

Keywords. Neutrinoless double beta decay; positron modes; deformed shell model; A=60–90 nuclei.

PACS Nos 23.40.Hc; 21.10.Tg; 21.60.Jz; 27.50.+e

1. Introduction

Double beta decay ($0\nu\beta\beta$) is a rare weak interaction process in which two identical nucleons inside the nucleus undergo decay with or without emission of neutrinos. The two-neutrino double beta decay is consistent with the standard model of electroweak interaction and has been observed in more than 20 nuclei. This process provides critical test of the goodness of nuclear models. On the other hand, neutrinoless double beta decay ($0\nu\beta\beta$) can occur only if neutrino is a Majorana particle and the conservation of lepton number is violated. Recent experimental measurements suggest that neutrinos have mass. Observations of $0\nu\beta\beta$ can give absolute neutrino mass provided the nuclear matrix elements are known from a reliable nuclear model. In view of the above, experimental programmes have been initiated at different laboratories across the globe to observe this decay. Except for a claim by Heidelberg–Moscow group for ^{76}Ge [1], this process has not yet been observed experimentally. The most recent experimental results are from

KamLAND-Zen [2] and EXO-200 [3] and they give the lower limit of 3.4×10^{25} yr. There has been considerable effort to obtain nuclear transition matrix elements (NTME) for various candidate nuclei and they have been calculated theoretically using a variety of nuclear models: (i) large-scale shell model, (ii) quasiparticle random phase approximation (QRPA) and its variants, (iii) proton–neutron interacting boson model (IBM-2), (iv) particle number and angular momentum projection including configuration mixing within the generating coordinate method framework (GCM+PNAMP), (v) projected Hartree–Fock–Bogoliubov (PHFB) method with pairing plus quadrupole–quadrupole interaction. Detailed comparative study of the results from these methods are discussed in [4]. All these calculations are focussed on the two-electron mode. However, it is possible to have neutrinoless positron double beta decay and this can come in three modes: (i) double β^+ ($\beta^+\beta^+$), (ii) β^+ and electron capture (β^+EC) and (iii) double electron capture (ECEC). All these three modes combined are referred to as 0ν e^+DBD. There are efforts to observe 0ν e^+DBD and some of the candidate nuclei are in A=60–90 region. These are ^{64}Zn, ^{74}Se, ^{78}Kr and ^{84}Sr [5–8]. To our knowledge, so far for these nuclei no calculations have been reported for NTME for 0ν e^+DBD.

^{64}Zn is a useful nucleus for studying double beta decay. Its natural isotopic abundance is 48.268%, which is quite large for a nucleus undergoing β^+ decay. As a result, it is possible to design experiments without isotopical enrichment thereby reducing the cost considerably. By taking a large mass of the sample because of its low cost, one can search for double beta decay processes successfully. Before going to double beta decay, we shall first study its spectroscopic properties using deformed shell model (DSM) to test the effectiveness of the model for this nucleus.

^{64}Zn and its daughter nucleus ^{64}Ni lie near the doubly magic nucleus ^{56}Ni. Near the ground state, most of the observed energy levels are shell model states. These nuclei also show collective bands. Because of these features, it is quite interesting to study these nuclei.

For the last many years, the DSM (based on Hartree–Fock states) has been used to study various properties of nuclei in the mass A=60–90 region (also in A=44–60) with considerable success [9–19]. More importantly, this model has also been used for studying 2ν double beta decay, in the first attempt, for ^{76}Ge $\rightarrow$ ^{76}Se in [20], half-lives for 2ν e^+DBD in ^{78}Kr in [21], in ^{74}Se [22] and in ^{84}Sr [23] with considerable success. In addition to these three nuclei, ^{64}Zn is also a candidate nucleus in the A=60–90 region.

In §2 the formula for half-life for 0ν e^+DBD and details of the DSM are given. Section 3 gives DSM results for ^{64}Zn for spectroscopic properties and then the results for both 2ν and 0ν positron double beta decay half-lives. Spectroscopic properties of ^{64}Zn and the daughter nucleus ^{64}Ni are studied using DSM for the first time in this paper. Finally, §5 contains conclusions.

2. Formalism

Half-life of 0ν e^+DBD for the 0_i^+ ground state (gs) of an initial even–even nucleus decay to the 0_f^+ gs of the final even–even nucleus is given by [24]

$$[T_{1/2}^{k:0\nu}(0_i^+ \rightarrow 0_f^+)]^{-1} = G^{0\nu}(k)(g_A)^4 \left|M^{0\nu}(0^+)\right|^2 \left(\frac{\langle m_\nu \rangle}{m_e}\right)^2 , \quad (1)$$

where $\langle m_\nu \rangle$ is the effective neutrino mass (a combination of neutrino mass eigenvalues and it also involves neutrino mixing matrix) and k denotes the $\beta^+\beta^+$ and β^+EC modes. The $G^{0\nu}(k)$ is the phase-space integral (kinematical factor) dependent on charge, mass and available energy for these two $0\nu\, e^+$DBD process. Improved values for these are given in [24] and these are used in the present work. It is important to note that 0νECEC can be considered as a resonant decay or a radiative process with or without resonance condition and this is discussed for ^{74}Se in [25]. In eq. (1) $M^{0\nu}$ is the nuclear transition matrix element (NTME) of the $0\nu\, e^+$DBD transition operator and it is a sum of a Gamow–Teller-like ($M_{\rm GT}$), Fermi-like ($M_{\rm F}$) and tensor ($M_{\rm T}$) two-body operators. It is well known that, the tensor part contributes only up to 10% of the matrix elements [4] and so we shall neglect the tensor part.

In DSM, for a given nucleus, starting with a model space consisting of a given set of single-particle (sp) orbitals and effective two-body Hamiltonian, the lowest energy intrinsic states are obtained by solving the Hartree–Fock (HF) single-particle equation self-consistently. Excited intrinsic configurations are obtained by making particle–hole excitations over the lowest intrinsic state. The HF intrinsic states $\chi_K(\eta)$, which is an anti-symmetrized product of the occupied deformed single-particle orbits (with K being the sum of k_i over occupied states), do not have definite angular momenta. The normalized states of good angular momentum are projected from these intrinsic states. It is easy to see that

$$\left\langle \chi_{K_1} | \mathrm{e}^{-i\beta J_y} | \chi_{K_2} \right\rangle = \det\left[M_{i\ell}(\beta) \right], \tag{2}$$

where

$$M_{i\ell}(\beta) = \sum_j c^{i*}_{jk_i} c^{\ell}_{jk'_\ell} d^j_{k_i\, k'_\ell}(\beta). \tag{3}$$

Here, i and ℓ stand for the deformed single-particle orbits. In general, the projected states with same J but from different intrinsic states will not be orthogonal to each other. Hence, they are orthonormalized and then band mixing calculations are performed.

The matrix elements of the operator $\mathcal{O}(2{:}0\nu)$ in the basis of these normalized states projected from different intrinsic states $\chi_K(\eta)$ can be written as

$$\mathcal{O}^J_{K\eta,K'\eta'} = \left\langle \psi^J_{MK}(\eta) \,|\, \mathcal{O} \,|\psi^J_{MK'}(\eta') \right\rangle \tag{4}$$

and they are given by

$$\mathcal{O}^J_{K\eta,K'\eta'} = \frac{2J+1}{2\sqrt{N_{JK} N_{JK'}}} \int_0^\pi \mathrm{d}\beta \, \sin\beta d^J_{KK'}(\beta) \left\langle \chi_K(\eta) | \mathrm{e}^{-i\beta J_y} \mathcal{O} | \chi_{K'}(\eta') \right\rangle. \tag{5}$$

The interaction kernel can be written as

$$\left\langle \chi_K | \mathrm{e}^{-i\beta J_y} \mathcal{O} | \chi_{K'} \right\rangle = \sum_{iki'k'} (-1)^{i+i'+k+k'} \left\langle ik | \mathrm{e}^{-i\beta J_y} \mathcal{O} | i'k' \right\rangle D^{n-2}_{ik,i'k'}, \tag{6}$$

where $D^{n-2}_{ik,i'k'}$ is the determinant of rank $(n-2)$ of the matrix elements given by eq. (3) obtained from the $n \times n$ determinant given in eq. (2) by removing the ith and kth rows and i'th and k'th columns. Expressing in basis states, we have

$$\langle \chi_K | e^{-i\beta J_y} \mathcal{O} | \chi_{K'} \rangle = \sum_{\alpha\gamma\alpha'\gamma'} \langle \alpha\gamma | e^{-i\beta J_y} \mathcal{O} | \alpha'\gamma' \rangle \, D^{n-2}_{\alpha\gamma,\alpha'\gamma'}. \tag{7}$$

Note that,

$$D^{n-2}_{\alpha\gamma,\alpha'\gamma'} = \sum_{iki'k'}^{n} (-1)^{i+k+i'+k'} C^{i*}_{\alpha} C^{k*}_{\gamma} C^{i'}_{\alpha'} C^{k'}_{\gamma'} D^{n-2}_{ik,i'k'} \tag{8}$$

and

$$\langle \alpha\gamma | e^{-i\beta J_y} \mathcal{O} | \alpha'\gamma' \rangle = \sum_{k_\delta k_{\delta'}} d^{j_\alpha}_{k_\alpha k_\delta} d^{j_\gamma}_{k_\gamma k_{\delta'}} \langle j_\alpha k_\delta, \, j_\gamma k_{\delta'} | \mathcal{O} | j_{\alpha'} k_{\alpha'}, \, j_{\gamma'} k_{\gamma'} \rangle \ . \tag{9}$$

For $0\nu e^+$DBD, the bra corresponds to the two-proton states and the ket corresponds to neutron states.

DSM is well established to be a successful model for transitional nuclei (A=60–90) when sufficiently large number of intrinsic states are included in the band mixing calculations. Performing DSM calculations for the parent and daughter nuclei and then using the DSM wave functions, the $\mathcal{O}(2{:}0\nu)$ operator matrix elements are calculated and the results are presented below.

3. Spectroscopic properties

As discussed in §2, we first carry out an axially symmetric HF calculation for each nucleus using the newly developed GXPF1A effective interaction [26] within the model space consisting of the orbitals $^1f_{7/2}$, $^2p_{3/2}$, $^1f_{5/2}$ and $^2p_{1/2}$ with ^{40}Ca as the core. The spherical single-particle energies for these orbits are taken as -8.6240, -5.6793, -1.3829 and -4.1370 MeV and are kept the same both for protons as well as neutrons. The lowest energy prolate and oblate solutions are shown in figures 1 and 2. For ^{64}Zn, the prolate and oblate solutions are nearly degenerate with the prolate solution slightly lower. There is a well-defined gap of more than 2 MeV above the proton Fermi surface and also above the neutron Fermi surface. As a result, ^{64}Zn has relatively stable deformation in ground state. On the oblate side, the proton gap is relatively small but the neutron gap is larger. As discussed before, particle and hole excitations over the lowest prolate and oblate solutions are considered to generate a total of 27 intrinsic states (with $K = 0^+$ and $K \neq 0^+$ upto 4 MeV excitation). Then, angular momentum projection from each of these intrinsic states is carried out and a band mixing calculation is performed. The calculated levels are classified on the basis of their $B(E2)$ values and structure of the levels.

In ^{64}Ni also, the prolate and oblate solutions are nearly degenerate with the oblate solution slightly lower. There are large proton gaps on prolate and oblate solutions. Hence, proton excitations over the Fermi surface are not expected to contribute significantly to the observed energy spectra. However, one can easily excite neutrons over the Fermi surface where the gap is low and generate excited configurations. We have considered 82 configurations with $K = 0^+$ and $K \neq 0^+$ upto 4 MeV excitation. Good angular

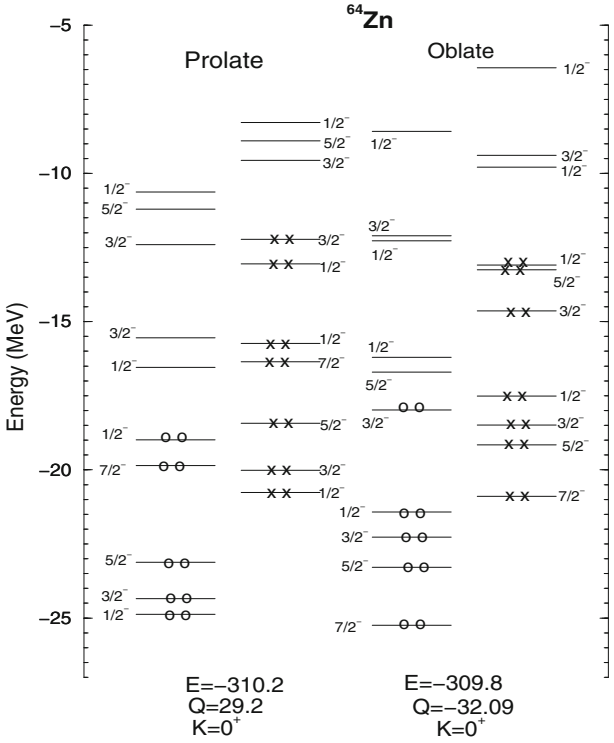

Figure 1. HF single-particle spectra for ^{64}Zn corresponding to the lowest prolate and lowest oblate configurations. In the figure, circles represent protons and crosses represent neutrons. The Hartree–Fock energy (E) in MeV, mass quadrupole moment (Q) in units of square of the oscillator length parameter and total K quantum number of the lowest intrinsic states are given in the figure. Each occupied single-particle orbital is two-fold degenerate because of time reversal symmetry.

momentum states are projected from each of these intrinsic states and then a band mixing calculation is performed to orthonormalize these projected states. The calculated levels having similar structure and connected by relatively large $B(E2)$ values are classified as belonging to one band.

The calculated levels and the bands for ^{64}Zn and ^{64}Ni are compared with the experiment in figures 3 and 4. The experiment data for the two nuclei are taken from [27–29]. The agreement is quite satisfactory. The ground band in both nuclei is mainly an admixture of the lowest prolate and oblate intrinsic configurations at low spin. However, at higher spins, there is mixing due to other configurations. The quasigamma band is also quite well reproduced in both the nuclei. There are many other energy levels which are compared with the experiment in figures 3 and 4. In addition to spectra, the $B(E2)$ values are also calculated with effective charge of e_p=1.5 and e_n=0.5. For ^{64}Ni, the calculated $B(E2)$ values for the transitions $2_1^+ \rightarrow 0_1^+$, $4_1^+ \rightarrow 2_1^+$, $0_2^+ \rightarrow 2_1^+$ and $4_2^+ \rightarrow 2_1^+$ are 7.5, 1.1, 2.1 and 1.0 compared to the experimental values 7.75±0.25, 6.7±1.1, 110±60 and 14±8 W.u., respectively. Similarly, for ^{64}Zn, the calculated $B(E2)$ values for these transitions are

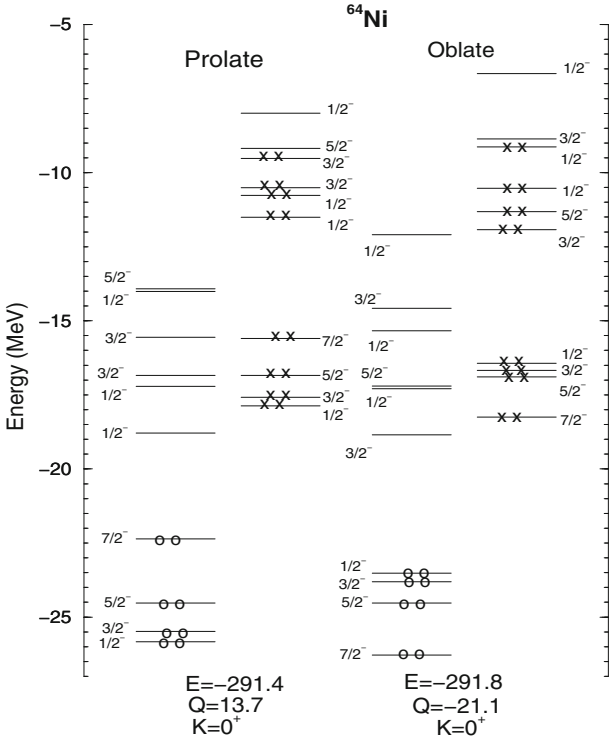

Figure 2. Same as in figure 1 but for ^{64}Ni.

20.7, 29.0, 2.40 and 0.58 compared to the corresponding experimental values 20.0±0.6, 12.2±0.05, 0.057±0.003 and 0.072±0.018, respectively. The experimental data are taken from [29]. In addition, many more $B(E2)$ transition probabilities have been calculated and the results will appear elsewhere. As seen from the above, DSM calculation reproduces the $B(E2)$ values satisfactorily.

Going beyond these, orbit occupancies for neutrons are compared with the DSM results in figure 5. Experimental data are taken from [30–32]. It is important to add that, there has been experimental efforts to measure the population of the valence orbits in several double beta decay candidate nuclei. This effort has been undertaken since theoretical calculations for the half-life of 0ν DBD are uncertain and hence, measurements of the occupation of valence orbits by protons and neutrons will provide a crucial test of the goodness of the model used to calculate the half-lives. The occupancies were recently measured by Schiffer *et al* using various single-particle transfer reactions [32–34]. It is seen from the results in figure 5 that within the experimental uncertainties, agreements between DSM and experimental results are good. In [32], neutron occupancy for $^1g_{9/2}$ is estimated as ∼0.6. However, in the present DSM calculation, this occupancy is absent as we are restricted only to $2p1f$ shell. With spectroscopic properties reasonably well reproduced by DSM, we have calculated e^+DBD half-lives using DSM wavefunctions and discuss these results below.

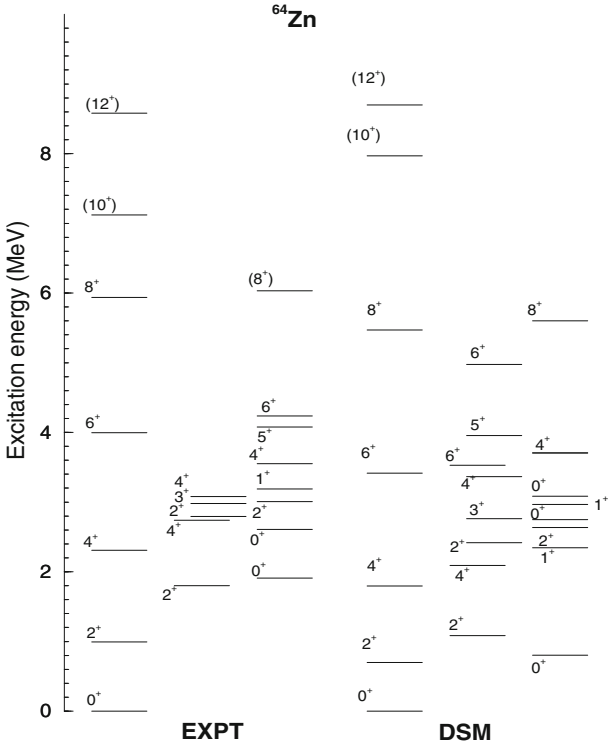

Figure 3. The calculated energy levels for ^{64}Zn are compared with the experiment. The experimental data are from [27] and [29].

4. $2\nu\ e^+$DBD half-lives and $0\nu\ e^+$DBD NTME and half-lives

First, we shall consider $2\nu\ e^+$DBD and the half-lives are given by

$$[T^{2\nu}_{1/2}(k, 0^+)]^{-1} = G_{2\nu}(k, 0^+)\left|M_{2\nu}(0^+)\right|^2, \tag{10}$$

where k denotes the modes $\beta^+\beta^+$, β^+ EC and ECEC. For ^{64}Zn, only the latter two modes are energetically possible. The kinematical factors $G_{2\nu}$ are independent of nuclear structure. Further, the NTME $M_{2\nu}$ are nuclear model-dependent and are given by

$$M_{2\nu}(0^+) = \sum_N \frac{\langle 0^+||\sigma\tau^-||1^+_N\rangle\langle 1^+_N||\sigma\tau^-||0^+_I\rangle}{[E_0 + E_N - E_I]}. \tag{11}$$

It is to be noted that for β^+ EC,

$$E_0 = \frac{1}{2}\left[M(A, Z) - M(A, Z-2) - 2m_e + e_{\rm b}\right] \tag{12}$$

and for ECEC

$$E_0 = \frac{1}{2}\left[M(A, Z) - M(A, Z-2) - 2m_e + e_{b_1} + e_{b_2}\right] \tag{13}$$

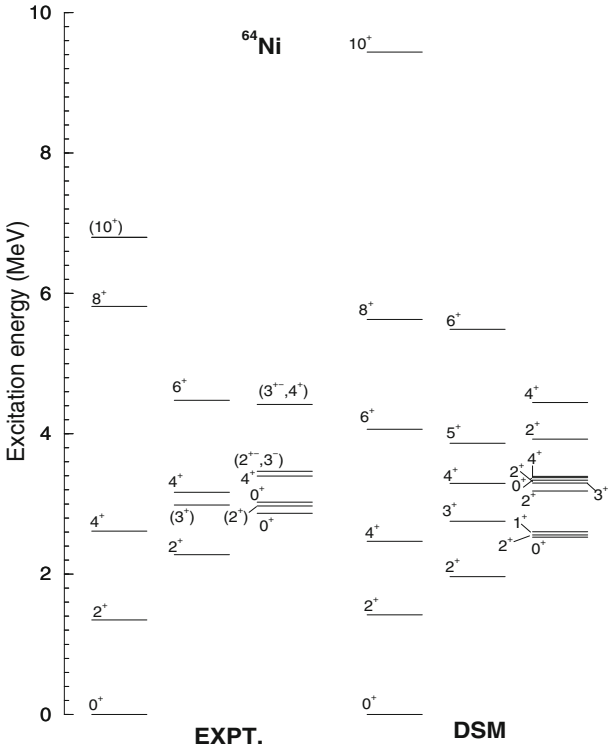

Figure 4. The calculated energy levels for ^{64}Ni are compared with the experiment. The experimental data are from [28] and [29].

Here, M denotes the neutral atomic mass taken from the table in [35] and e_b is the binding energy of the captured atomic K-electron.

In the DSM calculations, we have considered 10 lowest intrinsic states with $K = 0^+$ for ^{64}Zn, 34 lowest intrinsic configurations with $K = 0^+$ for the daughter nucleus ^{64}Ni and 48 intrinsic states with $K = 1^+$ for the intermediate nucleus ^{64}Cu. The intrinsic states with $K = 1^+$ for ^{64}Cu are generated by making particle–hole excitations over the lowest HF intrinsic state. Taking the phase-space factors $G_{2\nu}$ from the recent tabulated values given in [24] by Kotila and Iachello (3.81×10^{-33} yr^{-1} for β^+EC and 1.41×10^{-24} yr^{-1} for ECEC), the half-lives for the two cases come out to be 2.9×10^{36} yr and 7.9×10^{27} yr. These results are close to those obtained using single-state dominance hypothesis [36]. The calculated half-life for the ECEC mode can be taken as a useful prediction and it may be possible to observe this in future experiments. As discussed earlier, the main advantage of ^{64}Zn is its low cost so that a large mass of the sample can be taken.

Spectroscopic results and 2ν DBD half-lives given in table 1 show that we can use DSM for reliable predictions for 0ν e^+DBD. Turning to this, in the calculation of half-lives for 0ν e^+DBD we have considered 10 intrinsic states with $K = 0^+$ for ^{64}Zn and 34 intrinsic configurations with $K = 0^+$ for the daughter nucleus ^{64}Ni as in 2ν case. The calculated nuclear matrix element comes out to be 1.62. For ^{64}Zn, only β^+EC and ECEC are allowed

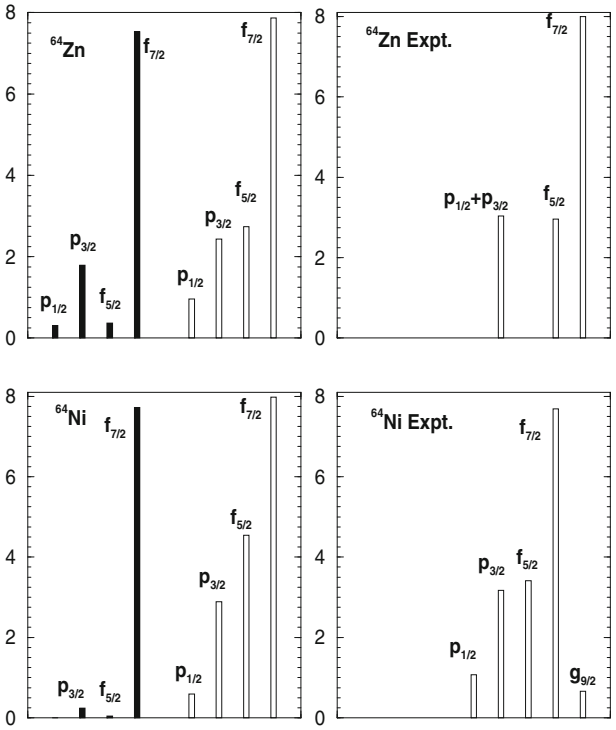

Figure 5. DSM results for occupancies of different orbits for ^{64}Zn and ^{64}Ni. Filled bars are for proton occupancies and open bars are for neutron occupancies. Results for neutron occupancies are compared with the experimental values given in [30–32].

energetically. However, the phase-space factor for ECEC is not yet known. Taking the neutrino mass to be 1 eV and the phase-space factor 5.07×10^{-20} yr^{-1} from [24], the calculated half-life for β^+EC is 7.24×10^{29} yr. At present, very low lower bounds for the half-lives are known from experiments for ^{64}Zn [5]. The DSM results for 0ν e^+DBD half-lives for the candidate nuclei in the mass region A=60–90 are summarized in table 2. The detailed results will be given elsewhere.

Table 1. DSM results for 2ν e^+DBD half-lives (yr) for nuclei with A=60–90.

Transition	$\beta^+\beta^+$	β^+EC	ECEC
$^{64}Zn \rightarrow {}^{64}Ni$		2.9×10^{36}	7.9×10^{27}
$^{78}Kr \rightarrow {}^{78}Se$	52.8×10^{25}	12.0×10^{22}	5.3×10^{22}
$^{74}Se \rightarrow {}^{74}Ge$		37.9×10^{30}	19.1×10^{22}
$^{84}Sr \rightarrow {}^{84}Kr$		1.2×10^{26}	4.2×10^{24}

Table 2. DSM results for 0ν e^+DBD half-lives with $m_\nu = 1$ eV. The values of $G^{0\nu}$ are taken from [24]. Note that the calculated nuclear matrix elements $M^{0\nu}$ are renormalized by a factor of 3.

	$\beta^+\beta^+$			β^+EC		
Nucleus	$G^{0\nu}$ (yr^{-1})	$M^{0\nu}$	$T_{1/2}$ (yr)	$G^{0\nu}$ (yr^{-1})	$M^{0\nu}$	$T_{1/2}$ (yr)
^{64}Zn				5.07×10^{-20}	4.86	8.04×10^{28}
^{74}Se				2.30×10^{-19}	1.56	1.70×10^{29}
^{78}Kr	2.5×10^{-18}	1.8	1.1×10^{28}	6.37×10^{-18}	1.8	4.70×10^{27}
^{84}Sr				1.94×10^{-18}	1.97	1.30×10^{28}

5. Conclusions

Prompted by recent experimental interest in 0ν e^+DBD of the four nuclei ^{64}Zn, ^{74}Se, ^{78}Kr and ^{84}Sr in A=60–90 region and the DSM results reported in [21–23] for the 2ν e^+DBD half-lives of ^{74}Se, ^{78}Kr and ^{84}Sr, we have first carried out spectroscopic calculations for ^{64}Zn as this nucleus was not studied before using DSM and then the NTME for 0ν e^+DBD are calculated. We have seen that DSM reproduces spectroscopic properties, including spectra, $B(E2)$s and occupancies, of the four candidate nuclei. In view of the above, the DSM half-lives for 0ν β^+EC (also $\beta^+\beta^+$ for ^{78}Kr) can be used as a guide for future experiments. We found that the calculated NTME has to be renormalized by a factor of 3. The detailed results for 0ν e^+DBD of ^{64}Zn, ^{74}Se, ^{78}Kr and ^{84}Sr will be published elsewhere.

Acknowledgements

RS is thankful to UGC and DST for the financial support. RS and VKBK thank F Iachello and M Horoi for useful discussions at European Centre for Theoretical Studies in Nuclear Physics and Related Areas (ECT*), Trento, Italy.

References

[1] H V Klapdor-Kleingrothaus and I V Krivosheina, *Mod. Phys. Lett. A* **21**, 1547 (2006)
[2] A Gando *et al*, *Phys. Rev. Lett.* **110**, 062502 (2013)
[3] M Auger *et al*, *Phys. Rev. Lett.* **109**, 032505 (2012)
[4] J Barea, J Kotila and F Iachello, *Phys. Rev. C* **87**, 014315 (2013)
[5] B P Belli *et al*, *J. Phys. G: Nucl. Part. Phys.* **38**, 115107 (2011)
[6] A S Barabash, P Hubert, A Nachab and V Umatov, *Nucl. Phys. A* **785**, 371 (2007)
[7] C Sáenz *et al*, *Phys. Rev. C* **50**, 1170 (1994)
[8] http://www.apctp.org/topical/2009/npap2009/Presentations/APCTP_NPAP2009_192_Kim.pdf
[9] R Sahu and S P Pandya, *J. Phys. G* **14**, L165 (1988)
[10] R Sahu and S P Pandya, *Nucl. Phys. A* **548**, 64 (1992)
[11] K C Tripathy and R Sahu, *J. Phys. G* **20**, 911 (1994)
[12] R Sahu and S P Pandya, *Nucl. Phys. A* **571**, 253 (1994)

[13] K C Tripathy and R Sahu, *Nucl. Phys. A* **597**, 177 (1996)
[14] K C Tripathy and R Sahu, *Int. J. Mod. Phys. E* **11**, 531 (2002)
[15] R Sahu and V K B Kota, *Phys. Rev. C* **66**, 024301 (2002)
[16] R Sahu and V K B Kota, *Phys. Rev. C* **67**, 054323 (2003)
[17] S Mishra, R Sahu and V K B Kota, *Prog. Theor. Phys.* **118**, 59 (2007)
[18] T S Kosmas, A Faessler and R Sahu, *Phys. Rev. C* **68**, 054315 (2003)
[19] R Sahu, K H Bhatt and D P Ahalpara, *J. Phys. G* **16**, 733 (1990)
[20] R Sahu, F Šimkovic and A Faessler, *J. Phys. G* **25**, 1159 (1999)
[21] S Mishra, A Shukla, R Sahu and V K B Kota, *Phys. Rev. C* **78**, 024307 (2008)
[22] A Shukla, R Sahu and V K B Kota, *Phys. Rev. C* **80**, 057305 (2009)
[23] R Sahu and V K B Kota, *Int. J. Mod. Phys. E* **20**, 1723 (2011)
[24] J Kotila and F Iachello, *Phys. Rev. C* **87**, 024313 (2013)
[25] V S Kolhinen *et al*, *Phys. Lett. B* **684**, 17 (2010)
[26] M Honma, T Otsuka, B A Brown and T Mizusaki, *Phys. Rev. C* **69**, 034335 (2004)
[27] D Karlgren *et al*, *Phys. Rev. C* **69**, 034330 (2004)
[28] R Broda *et al*, *Phys. Rev. C* **86**, 064312 (2012)
[29] ENSDF Data Base, Brookhaven National Laboratory, USA, http://www.nndc.bnl.gov/ensdf/index.jsp
[30] D von Ehrenstein and J P Schiffer, *Phys. Rev.* **164**, 1374 (1967)
[31] V K B Kota and V Potbhare, *Nucl. Phys. A* **331**, 93 (1979)
[32] J P Schiffer *et al*, *Phys. Rev. Lett.* **108**, 022501 (2012)
[33] J P Schiffer *et al*, *Phys. Rev. Lett.* **100**, 112501 (2008)
[34] B P Kay *et al*, *Phys. Rev. C* **79**, 021301(R) (2009)
[35] G Audi, A H Wapstra and C Thibault, *Nucl. Phys. A* **729**, 337 (2003)
[36] P Domin, S Kovalenko, F Šimkovic and S V Semenov, *Nucl. Phys. A* **753**, 337 (2005)